

Activation of oxide-ion conduction in KNbO₃ by addition of Mg²⁺

著者	Li Liping, Li Guangshe, Smith R. L., Inomata H.
journal or publication title	Applied Physics Letters
volume	81
number	15
page range	2899-2901
year	2002
URL	http://hdl.handle.net/10097/51557

doi: 10.1063/1.1512957

Activation of oxide-ion conduction in KNbO_3 by addition of Mg^{2+}

Liping Li^{a)}*Department of Physics, Jilin University, Changchun 130023, People's Republic of China*Guangshe Li,^{b)} R. L. Smith, Jr., and H. Inomata*Research Center of Supercritical Fluid Technology, Department of Chemical Engineering, Tohoku University, Sendai 980-8579, Japan*

(Received 28 February 2002; accepted 15 August 2002)

Niobate perovskite oxides of $\text{KNb}_{1-x}\text{Mg}_x\text{O}_{3-\delta}$ were synthesized directly at high temperature and pressure. X-ray diffraction confirmed the formation of single-phase orthorhombic structures. High-temperature Raman spectroscopy in combination with thermal analysis showed that phase transitions occurred from orthorhombic to tetragonal, to pseudo cubic, and finally to cubic, in sequence. Addition of Mg^{2+} at the Nb^{5+} sites of perovskite KNbO_3 lattice led to a dramatic enhancement of oxide-ion conduction. This enhancement in oxide-ion conduction was through the suppression of the contribution from p -type holes, which shows that these high-temperature phases can be promising candidates as conductive materials. © 2002 American Institute of Physics. [DOI: 10.1063/1.1512957]

Niobate-based perovskite oxides are of great interest to the physics community, since these materials have physical properties that are highly dependent on structure.¹ For example, rhombohedral ferroelectric KNbO_3 transforms to a paraelectric cubic phase at high temperatures¹ and by structural modification, the properties of KNbO_3 can be further tailored for specific applications. The K^+ -site substitutions by elements such as Ba^{2+} can yield semiconducting behavior,² while substitutions at the Nb^{5+} site with Mg^{2+} enhance optical properties.³ Niobate-based perovskite oxides such as $\text{PbMg}_{1/3}\text{Nb}_{2/3}\text{O}_3$ show dielectric enhancements, while their ionic conduction is poor. Research on Mg^{2+} doping at the octahedral site shows enhanced ionic conduction in perovskite lattices.^{4,5} If oxide-ion conduction can be activated and phase transitions can be modified by doping KNbO_3 , then this could open the door to a new technological era.

Current perovskite lattices with Mg^{2+} and Nb^{5+} simultaneously at octahedral sites have to be prepared through two-step sintering processes that have MgNb_2O_6 as the key intermediate phase. It is of great interest to develop a single-step route to highly crystallized Mg niobate-based perovskite oxides and to determine the oxide-ion conduction enhancement in these lattices.

In this letter, we report on a single-step synthesis and oxide-ion conduction of $\text{KNb}_{1-x}\text{Mg}_x\text{O}_{3-\delta}$ that was obtained by high-temperature and high-pressure conditions.

The synthesis of $\text{KNb}_{1-x}\text{Mg}_x\text{O}_{3-\delta}$ was achieved with the following procedure. KHCO_3 , MgO , and Nb_2O_5 were used as the starting materials, and were grinded fully at molar ratios of $\text{K} : \text{Nb} : \text{Mg} = 1 : 1-x : x$ with $x = 0.05-0.30$. This mixture was placed into a high-pressure chamber as described in our previous article.⁶ Pressure was set to 4.0 GPa and then the temperature was increased gradually to

870 °C. After maintaining these conditions for 40 min, the specimens were quenched to room temperature under high pressure and subsequently, the pressure was released.

X-ray diffraction (XRD) data of samples were measured at room temperature at a scan rate of $0.3^\circ 2\theta/\text{min}$. The lattice parameters for the samples were calculated by least-squares methods. Phase transitions were determined by high-temperature Raman spectroscopy. Phase transitions were determined by differential thermal analysis (DTA). The ionic conductivities for the pellet samples were measured using ac impedance spectroscopy with an alternating current at a frequency between 10 Hz and 9 MHz at an amplitude of 50 mV in the temperature range of 400–800 °C in air. The impedance spectra were also measured at different oxygen partial pressures.

XRD data (Fig. 1) of the samples $\text{KNb}_{1-x}\text{Mg}_x\text{O}_{3-\delta}$ consisted of several split diffraction peaks, indicating a low symmetric structure. The double lines that can be observed at $\sim 23^\circ$ and 47° are characteristic of the orthorhombic perovskites. The XRD patterns were scaled for $x < 0.30$ but this did not result in any weak peaks arising from MgNb_2O_6 or $\text{Mg}_4\text{Nb}_2\text{O}_9$. These phases are, however, key intermediates during the formation of Mg niobate-based perovskite oxides.⁷ These results clearly demonstrated that high-temperature and high-pressure conditions provided a single-step synthesis route to orthorhombic perovskite lattice $\text{KNb}_{1-x}\text{Mg}_x\text{O}_{3-\delta}$.

The substitution of Mg^{2+} at the Nb^{5+} sites was also evident from the diffraction peak shifts under the lattice volume variation. The lattice volume increased with the dopant content of Mg^{2+} (inset of Fig. 1) mainly due to Mg^{2+} being larger than Nb^{5+} in octahedral coordination. Doping Mg^{2+} at Nb^{5+} sites would most likely produce a larger lattice distortion for lattice expansion. The large charge difference between Nb^{5+} and Mg^{2+} may produce some negative charge centers on a local scale around Mg^{2+} , since this would have to be balanced by oxygen vacancies. Each two Mg^{2+} ions should yield three oxygen vacancies V_{O} , which would be attracted to the nearest neighboring positions of Mg^{2+} under

^{a)}Present address: Department of Materials Science and Engineering, California Institute of Technology, Pasadena, California 91106.

^{b)}Author to whom correspondence should be addressed; present address: C302 BNSN, Department of Chemistry and Biochemistry, Brigham Young University, Provo, UT 84604; electronic mail: guangshe@hotmail.com

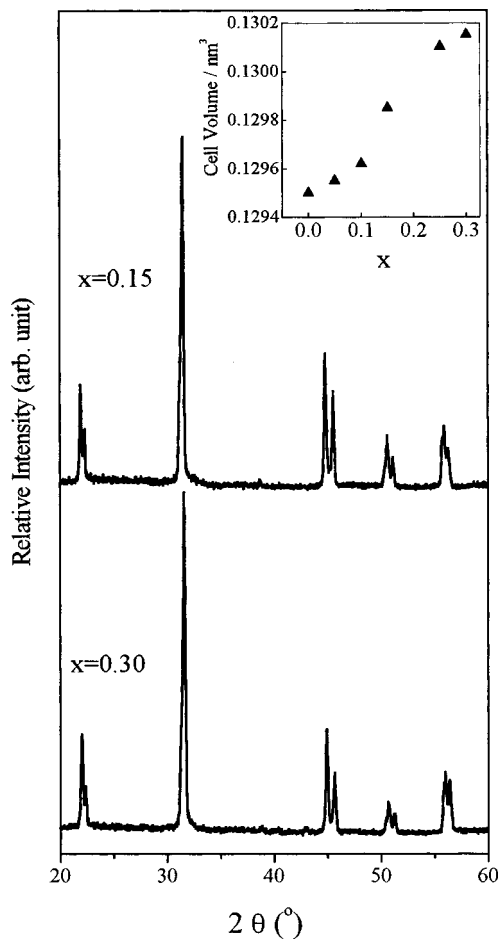


FIG. 1. XRD patterns for $\text{KNb}_{1-x}\text{Mg}_x\text{O}_{3-\delta}$ at typical compositions $x = 0.15$ and 0.30 . Inset illustrates the variation of the lattice volume with dopant content.

Coulombic forces. In our samples, the concentration of oxygen vacancy V_{O} would increase with Mg^{2+} content. The cationic substitutions and variations for the relative content of oxygen vacancy V_{O} and defect associations $\{\text{Mg}_{\text{Nb}}^{\text{III}}V_{\text{O}}\}$ were, therefore, assumed to be the main factors for the increase in lattice volume. This follows similar reasoning as that has been proposed to explain the nonlinearity for solid solutions of $\text{Ce}_{1-x}\text{RE}_x\text{O}_{2-x}$ ($\text{RE} = \text{Eu}, \text{Tb}$).⁸

Figure 2 shows Raman spectra for $\text{KNb}_{0.85}\text{Mg}_{0.15}\text{O}_{2.78}$ at given temperatures. The Raman spectra recorded at temperatures below 150°C were nearly the same as those of undoped KNbO_3 .⁹ When the temperature was increased to 200°C (Fig. 2), the intensity for the weak sharp phonon mode at 190 cm^{-1} was decreased, and the mode at $\sim 280\text{ cm}^{-1}$ became asymmetric due to asymmetric $\text{Nb}(\text{Mg})\text{O}_6$ octahedra at B sites,¹⁰ indicating that the orthorhombic phase was not predominant. The phonon mode at 530 cm^{-1} vanished, while the mode at $\sim 580\text{ cm}^{-1}$ exhibited a single mode of high symmetry. With an increase in temperature, the weak sharp phonon mode associated with the orthorhombic structure disappeared at $\sim 190\text{ cm}^{-1}$ and the phonon modes centered at ~ 280 and 580 cm^{-1} became two symmetric modes, while the mode at $\sim 830\text{ cm}^{-1}$ was further weakened. A tetragonal phase was formed at a temperature above 200°C . The phase transition of orthorhombic to tetragonal corresponded to an endothermic process, as indicated by the thermal peak at 203°C in the DTA curve

(inset of Fig. 2). When the temperature was increased to 400°C , the mode at $\sim 830\text{ cm}^{-1}$ lost most of its intensity, indicating the formation of a pseudo-cubic phase.¹¹ The phase transition of tetragonal to pseudo cubic was also endothermic, as demonstrated by the thermal peak at 378°C in DTA (inset of Fig. 2). At temperatures above 500°C , both phonon modes at ~ 280 and 580 cm^{-1} further broadened and lost intensity, which could be associated with the transition of pseudo cubic to cubic. Above 600°C , both phonon modes further weakened at ~ 280 and 580 cm^{-1} . The mode at $\sim 830\text{ cm}^{-1}$ disappeared completely. These results are evidence for the formation of a cubic phase.¹² The thermal effect for the phase transition of pseudo cubic to cubic is not obvious. Similar phase transitions were also observed at other compositions in $\text{KNb}_{1-x}\text{Mg}_x\text{O}_{3-\delta}$.

The transition from tetragonal to pseudo cubic could be associated with the change from tetragonal mode to triply degenerated cubic F_{1u} mode. KNbO_3 modified by larger Mg^{2+} substitution could give a large displacement for Nb^{5+} , and the oxygen vacancies adjacent to Mg^{2+} could produce distorted polyhedra around Nb^{5+} . Pseudo-cubic $\text{KNb}_{1-x}\text{Mg}_x\text{O}_{3-\delta}$ contained a partial lattice order, whereas B -site ions in the cubic phase are assumed to be distributed disorderly at eight off-center sites along the $\langle 111 \rangle$ axes due to the potential-energy minima at these sites.¹³ The presence of these Raman modes confirmed some disordered arrangements in the lattice. Similar distributions of Mg^{2+} and Nb^{5+} can probably be expected at one to eight off-center sites along the $\langle 111 \rangle$ axes in the presence of some lattice distortions due to the size mismatch of $\text{Mg}^{2+}/\text{Nb}^{5+}$. Further, oxygen vacancies or oxygen vacancy clusters adjacent to Mg^{2+} could give rise to an inhomogeneous distribution of the electrical field at B sites. The different static displacements of Mg^{2+} and Nb^{5+} decreased the local symmetry around B site ions. With increasing temperature, a rapid increase in the disorder of $\text{Nb}^{5+}/\text{Mg}^{2+}$ at B sites favored preservation of the highly symmetric average cubic structure at high temperature. Large amounts of oxygen vacancies V_{O} and defect associations $\{\text{Mg}_{\text{Nb}}^{\text{III}}V_{\text{O}}\}$ at higher dopant contents exhibited strong interactions with the framework ions and mobile oxygen ions. The transition of order-disorder of oxygen vacancies was thus suppressed.

The impedance spectra clearly showed bulk and grain boundary conduction as well as electrode polarization (not shown). The total conductivity data derived from the impedance spectra were separated into two linear regions, corresponding to the high-temperature phases, respectively (Fig. 3). The ionic conduction at lower temperatures showed a lower activation energy of 0.58 eV at 500°C at $x = 0.1$, while above the transition temperatures, there was a break in the conductivity data showing an increase in the activation energy to 0.83 eV at temperatures greater than 700°C . Theoretical modeling reported in the literature¹⁴ has noted oxidation or cation conduction in perovskite lattices. However, for the present samples, cation conduction associated with K^+ , Mg^{2+} , and Nb^{5+} is most unlikely to occur via cation vacancies. This can be reasoned from the comparison of the measured activation energies and the theoretical values for cation conduction. The activation energies of our samples were relatively lower having values of around 1.0 eV , which is

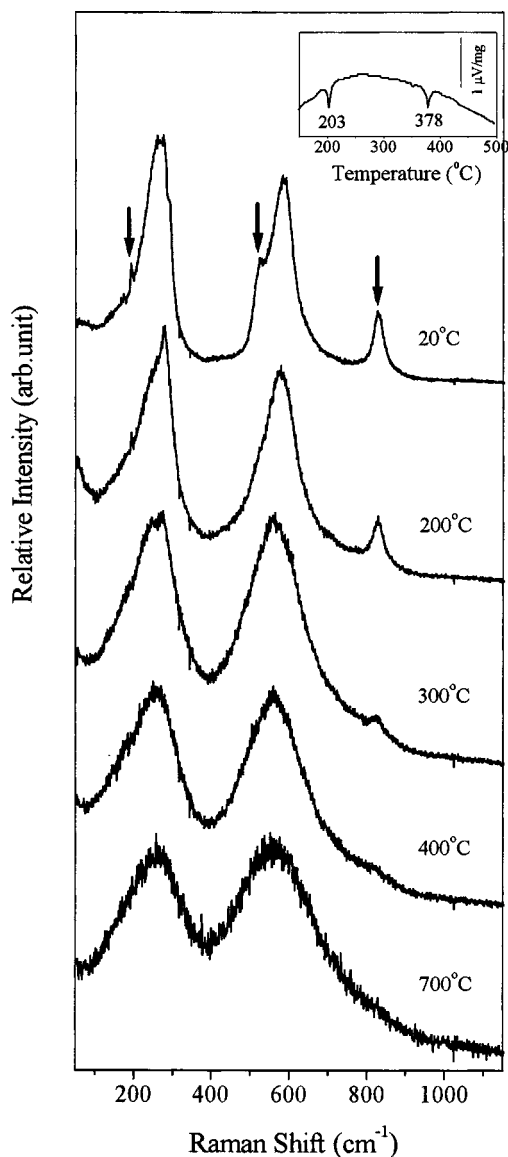


FIG. 2. Raman spectra for $\text{KNb}_{0.85}\text{Mg}_{0.15}\text{O}_{2.78}$ at the given temperatures. Inset shows a DTA curve that demonstrates the endothermic nature of the phase transitions from orthorhombic to tetragonal at 203 °C and to pseudo cubic at 378 °C.

characteristic for migration of oxygen vacancies. Assuming cation conduction was present in the samples, the extremely large ionic size of 1.64 Å for K^+ at A site would probably yield an activation energy larger than 4.0 eV.¹⁴ For the B-site ions such as Mg^{2+} and Nb^{5+} , the migration energy along the diagonal direction $\langle 110 \rangle$ would be even higher and would have a value, most likely, around 14 eV. Therefore, cation vacancy formation and, furthermore, cation conduction by vacancy migration between the neighboring sites should be highly unfavorable as expected for the close-packed perovskite lattice. The conductivity data for a typical sample of $\text{KNb}_{0.90}\text{Mg}_{0.10}\text{O}_{2.85}$ were measured at 500 °C under several oxygen partial pressures around that of air (Fig. 3, inset). No pronounced variations were observed in conductivity, which shows the ionic nature of primary oxide-ion conduction. Even though there was a small increase in the conductivity at higher oxygen partial pressures, the slope $\partial \log \sigma / \partial \log PO_2$ in this oxygen partial pressure region was much smaller than

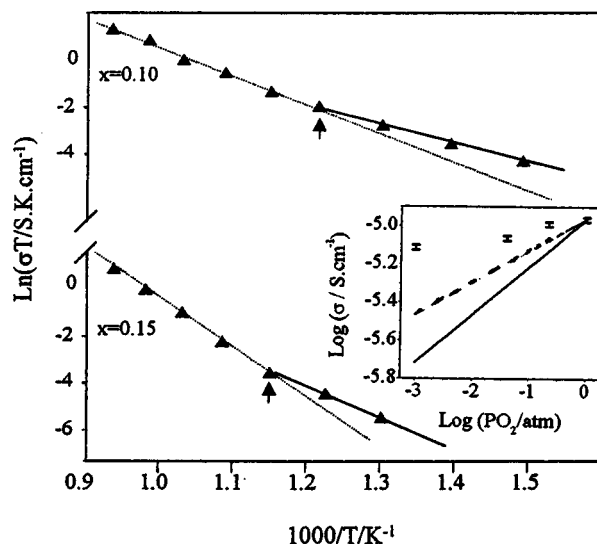


FIG. 3. Temperature dependence of total conductivity for $\text{KNb}_{1-x}\text{Mg}_x\text{O}_{3-\delta}$ at $x=0.10$ and 0.15 . Inset shows the conductivity dependence on oxygen partial pressure at 500 °C for $x=0.10$.

1/4 or 1/6, which makes it likely that the p -type electronic contribution is extremely small in this region.¹⁵ The ionic conductivity data varied systematically with the dopant content and can be associated with the relative content of oxygen vacancies and defect associations as well as the order-to-disorder transitions, and will be described elsewhere. $\text{KNb}_{0.90}\text{Mg}_{0.10}\text{O}_{2.85}$ was determined to exhibit the most favorable conduction characteristics such as a relatively high conductivity ($\sigma_{700^\circ\text{C}} = 1.10 \times 10^{-3} \text{ S cm}^{-1}$) and low activation energy ($E_a = 0.83 \text{ eV}$).

This project is financially supported by a fund from NSFC (No.19804005) (L.L.). G.L. thanks Dr. S. Haile at Caltech for access to oxygen partial pressure impedance measurements.

- ¹M. D. Fontana, G. Metrat, J. L. Servoin, and F. Gervais, *J. Phys. C* **16**, 483 (1984); R. Sommer, N. K. Yushin, and J. J. van der Klink, *Phys. Rev. B* **48**, 13230 (1993); D. L. Orattapong, J. Toulouse, J. L. Robertson, and Z. G. Ye, *Phys. Rev. B* **64**, 212101 (2001).
- ²D. Hamada, M. Machida, Y. Sugahara, and K. Kuroda, *J. Mater. Chem.* **6**, 69 (1996).
- ³L. E. Busse, L. Goldberg, M. R. Surette, and G. Mizell, *J. Appl. Phys.* **75**, 1102 (1994).
- ⁴K. Q. Huang and J. B. Goodenough, *J. Alloys Compd.* **303**, 454 (2000).
- ⁵S. M. Choi, K. T. Lee, S. Kim, M. C. Chun, and H. L. Lee, *Solid State Ionics* **131**, 221 (2000).
- ⁶D. Lu, L. Li, J. Miao, H. Liu, and W. Su, *Rev. High Pressure Sci. Technol.* **7**, 1031 (1998).
- ⁷S. L. Swartz and T. R. Shrout, *Mater. Res. Bull.* **17**, 1245 (1982).
- ⁸L. Li, G. Li, Y. Che, and W. Su, *Chem. Mater.* **12**, 2567 (2000).
- ⁹A. M. Quittet, M. I. Bell, M. Krauzman, and P. M. Raccach, *Phys. Rev. B* **14**, 5068 (1976).
- ¹⁰I. J. Clark, T. Takeuchi, N. Ohtori, and D. C. Sinclair, *J. Mater. Chem.* **9**, 83 (1999).
- ¹¹M. D. Fontana, G. E. Kugel, J. Vamvakas, and C. Carabatos, *Solid State Commun.* **45**, 873 (1983).
- ¹²M. D. Fontana and M. Lambert, *Solid State Commun.* **10**, 1 (1972).
- ¹³T. P. Dougherty, G. P. Weidnerrecht, K. A. Nelson, M. H. Garrett, H. P. Jenssen, and C. Warde, *Phys. Rev. B* **50**, 8996 (1994).
- ¹⁴M. S. Islam, *J. Mater. Chem.* **10**, 1027 (2000).
- ¹⁵T. Shimura, S. Fujimoto, and H. Iwahara, *Solid State Ionics* **143**, 117 (2001).